JOURNAL OF PROPULSION AND POWER
Vol. 24, No. 2, March–April 2008

Slight-Premixing Effects on Oxidation/Formation of Polycyclic Aromatic Hydrocarbon in Counterflow Flames

Yuji Nakamura*
Hokkaido University, Sapporo 060-8628, Japan
and
Daisuke Ishii,† Shingo Satake,† and Hiroshi Yamashita‡
Nagoya University, Nagoya 464-8603, Japan

DOI: 10.2514/1.20998

This paper considers experimentally the effect of the oxygen addition to the fuel flow given to the oxidation/formation characteristics of polycyclic aromatic hydrocarbon (PAH) in a methane–air, counterflow, nonpremixed (diffusion) flame. The amount of oxygen added in the fuel flow is 0.0–15.0% of range in a volumetric flow rate, and a corresponding equivalence ratio is 10 or more. A quartz microsampling probe was inserted into the flame to extract the test gas, and the local amount of lighter hydrocarbons including three or four carbons (C3 and C4, respectively), and PAH was investigated using a gas chromatograph-mass spectrometer. Distribution of temperature, the emissive power (near 650 nm) of a luminous flame, and OH fluorescence intensity were separately measured. On the conditions used in this experiment, it turned out that soot yield and detected PAH mole fraction decreased with the increase in the added amount of oxygen. The depletion degree became weaker gradually and their inhibition by an oxygen addition was reaching the ceiling. Additionally, the peak in the profile of the mole fraction of PAH approached the elevated-temperature zone with an increase in the added amount of oxygen. These results suggest that the promotion of PAH formation is somehow associated with the increase in temperature. The reason for such leveling off is considered as follows. Oxidation of the benzene in the fuel flow is promoted by the increase in the added amount of oxygen, and the components of C3 and C4 are produced. If these arrive at the elevated-temperature zone, oppositely, benzene is produced via C3 and C4. Consequently, a difference will be lost in the total amount of PAH generated.

Nomenclature

$[OH]_{fl}$	=	fluorescence intensity of OH radical, a.u.
T	=	field temperature, K
Xi	=	mole fraction of ith species, ppm
x	=	oxygen fraction added to the fuel flow
z	=	distance from lower (fuel side) nozzle, mm

I. Introduction

PARTICULATE matter (PM) is one of the harmful combustion products which mainly consist of unburned carbon (soot), and the amount-of-emission reduction is an urgent subject. To control the emission clearance, a diesel particulate filter (DPF) is often used as a means for reducing PM delivery from an automobile. A finer filter is capable of capturing the smaller PM. However, an entire removal of small PM (PM2.5, known as lung cancer matter) is still a challenging matter, because pressure loss will increase and energy conversion efficiency will fall with an extensively finer filter. To attain energy savings and clean emission simultaneously, it is more desirable to reduce PM *during* a combustion process rather than removing by aftertreatment. The simplest way is to do a seeding oxidizing compound into the fuel flow to burn PM and polycyclic aromatic hydrocarbon (PAH, which is known as the precursor of soot) in the combustion zone. However, in the case of the fuel-enriched combustion, an oxygen addition into the system causes an increase in the flame temperature and PAH, and eventually soot formation would be enhanced because of it. In this sense, an oxygen addition may not always be an effective way to reduce PM/PAH: there must be an appropriate condition to work with such an approach. The aim of the present study is to elucidate the oxidation/formation character of PAH (one and two rings) in various slightly premixed conditions (a small amount of oxygen added into the fuel flow).

Soot is formed in the flame under a fuel-enriched condition through complicated processes. The schematic diagram of a typical soot formation path is shown in Fig. 1. A comparatively light hydrocarbon component makes a carbon number increase through pyrolysis, and after it goes via PAH [1–8], it forms the primary particle (a typical diameter is tens of nm) of soot with an inner core and outer shell structure [9]. During the process, the role of PAH is crucially important [10], and it is indispensable to predict a soot yield to understand a PAH formation process correctly [11].

Much investigation on the formation process of PAH has been made, and knowledge about the connection between C2/C3/C4 components and PAH has been acquired [12–30]. The formation of benzene, which is the fundamental unit of PAH, is considered by the following three reactions: 1) the reaction of C2 and C4 [12], 2) recombination reaction of a propargyl radical (C3H3) [13,15,18], and 3) the reaction in which the other C3 participates [30]. It has been reported that the importance of the reaction of 1 changes with fuels [27]. Based on the rich knowledge, a variety of chemical reaction models have been proposed for a premixed flame [15–17] as well as a nonpremixing (diffusion) flame [24,26], including C2/C3/C4 components and PAH. Every model does an excellent job of predicting the generated PAH (to their mole fraction profiles) for the specified conditions; however, it is still difficult to do in all flames with *one* certain model. This is reflecting the facts which are not fully understood about the difference in the PAH formation/oxidation characteristics in a premixed flame and a nonpremixing (diffusion) flame, that is, the role of the oxygen given to a PAH formation/oxidation process.

Presented at the International Symposium on EcoTopia Science 2005 (ISETS05), Nagoya, Japan, 8–9 August 2005; received 8 November 2005; revision received 26 April 2007; accepted for publication 31 July 2007.

*Associate Professor, Division of Mechanical and Space Engineering, N 13 W 8 Kita-ku.
†Graduate Student, Department of Mechanical Science and Engineering, Furo-cho, Chikusa-ku.
‡Professor, Department of Mechanical Science, Furo-cho, Chikusa-ku.

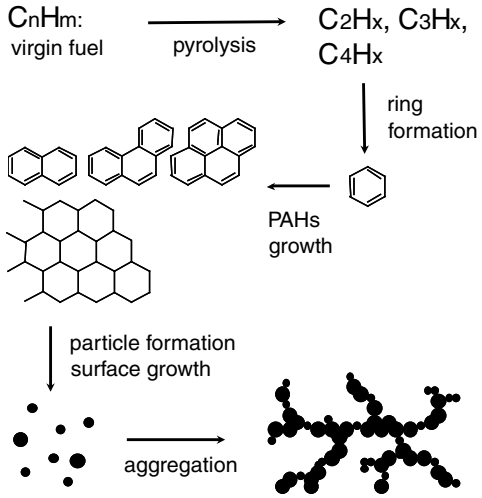

Fig. 1 Schematic diagram of PAH and soot formation processes.

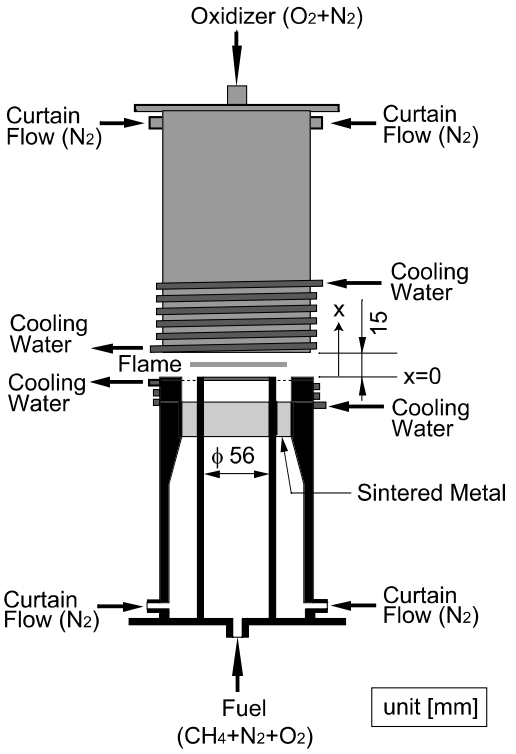

Fig. 2 Schematic illustration of the counterflow burner system.

Two different ways are considered about the effect of the oxygen given to a PAH formation/oxidation process. One is to promote PAH formation/growth via a five-member ring radical (C5H5, cyclopentadienyl) [17,23,28,29] (although there is a report that cyclopentadienyl is not important with a nonpremixed flame for PAH formation [26]), and the other is simply to be consumed by oxidation [5,14,16,25,28,29]. For the partial premixed flame, McEnally et al. [19–22] investigated in detail the formation characteristics of PAH and soot with various fuels and initial conditions in the coaxial jet burner. According to their findings, the generated amount of PAH and soot decreases monotonically as the amount of seeded oxygen was increased (the condition was approached to the premixed combustion). However, by adopting the coaxial jet burner, a considerable amount of oxygen naturally flows into the fuel side from the quenched zone formed between a flame base and a burner rim, and the precise amount of oxygen which participated in burning is ambiguous. In addition, although they were examining using the distribution on a center axis, it is difficult to carry out comparison analyses with other conditions because the multidimensional effect must be considered. To investigate the effect of the oxygen additive and eliminate the effect of a multidimensional nature, it is desirable to use a one-dimensional flame.

For PAH analysis in the flame, we developed the direct-sampling measurement system [31–33]. In previous work, we studied the effects of a benzene addition in fuel flow [31] and the oxygen amount in an *oxidizer* on PAH formation [32,33]. It has been understood that an additional slight aromatic compound does not change the major flame structure and also gives a minor role on enhancement of PAH formation. Oppositely, an increase in the oxygen amount in the oxidizer flow gives higher PAH formation. It is suspected that this might be due to the elevated flame temperature which could enhance the pyrolysis in the fuel side to open reaction pathway to form PAH. These results imply that the flame temperature and its profile are quite important in determining the PAH formation/destruction processes in the flame. Generally, it has been said that the oxygen addition into the *fuel* flow could reduce the soot and PAH via their oxidation; however, if a premixing increases flame temperature, there is no guarantee to let that happen. In this sense, a detailed study of PAH behavior with a slightly premixing condition is important.

This study aims at understanding the role of oxygen in the fuel flow on PAH formation/oxidation characteristics by investigating the change of profiles in C3/C4 components and PAH for a counterflow, methane–air nonpremixing (diffusion) flame. The added amount of oxygen to a fuel flow is 0.0–15.0% by volume, and a corresponding equivalence ratio is 10 or more. A quartz microsampling probe is inserted in an object flame, and the local test gas is extracted to analyze through a gas chromatograph-mass spectrometer (GCMS). In our GCMS system, in addition to C3 and C4 components, it is detectable to PAH of four rings [31], but an argument only up to two rings will be made here. In addition to measuring the concentration profiles of C3/C4 components and PAH, profiles in temperature (based on a thermocouple), luminescence intensity (based on a camera with a filter) of a luminous flame, and relative OH radical concentration (LIF, based on laser-induced fluorescence) are also measured, and the role of the oxygen addition given to PAH formation/oxidation characteristics is examined in detail.

II. Experiments

A. Burner Systems

The schematic diagram of the counterflow burner used in this study is shown in Fig. 2. This burner is the same as what was used in our past studies [31–33]. One pair of cylinder burners gives a stagnation point flowfield. Each burner is a coaxial burner: the outside surroundings flow encloses the inside mainstream. The water-cooled jacket is attached on the outer surface to prevent the rise in temperature of a burner and internal gas. To make the ejected flow uniform, the sintering metal is installed in the outlet of the burner. From the mainstream of a lower nozzle and an upper nozzle, fuel gas (mixture of CH4/O2/N2) and oxidizer gas (mixture of N2/O2) are ejected, respectively, and the steady, flat, one-dimensional, nonpremixing (diffusion) flame is formed between nozzles. Nitrogen is used for a surrounding flow of upper and lower nozzles to protect a flame from external turbulence, if any. The distance between two burners is fixed to 15 mm, and the mainstream velocity is fixed to 6.0 cm/s (at room temperature). Although the water-cooled system is attached, the burner surface is not always cooled to room temperature. Therefore, the actual velocity near the surface would be higher than 6.0 cm/s. A mass flow controller (STEC SEC-E 40/50) is used to control every flow rate, and an authentication flow rate error is 0.5%.

Direct photographs of typical counterflow, methane–air nonpremixing (diffusion) flames are shown in Fig. 3. On the left, the case without the oxygen addition is shown, while on the right, the case with 15% oxygen addition (in the fuel flow, corresponding equivalence ratio is 10) is shown. Although a slight bending of a luminous flame is observed at both ends, one can confirm that the uniform (flat) flame is formed near the center part. It is hard to identify a difference to the brightness of a luminous flame visually;

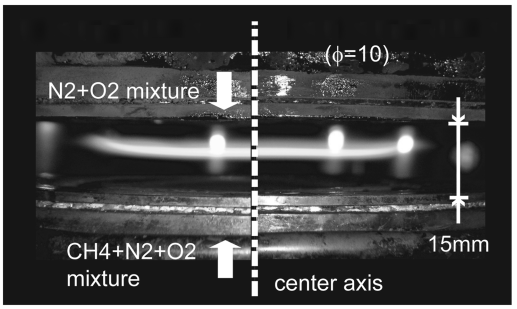

a) Nonpremixed b) Slightly premixed

Fig. 3 Direct photographs of represented 1-D flames considered in the present study. a) No oxygen addition; b) 15% of oxygen addition into the fuel flow.

however, it turns out that in the right flame (the case with the oxygen addition), the thickness of the luminous flame becomes thinner than the other (the case without the oxygen addition).

B. Gas-Analyzing System

The schematic diagram of a GCMS analyzing system is shown in Fig. 4. Again, these are the same as what was used in our past studies [31–33]. A quartz microsampling probe (inner diameter of about 0.2 mm) is attached in the end of a gas path to be inserted in a flame horizontally to perform gas sampling. Two gas paths are arranged in this system, with one path leading to a vacuum pump and the other path leading to a GCMS analyzer (Shimazu GC-17A ver. 3 GC-MS QP 5050A). All gas paths are kept at 550 K by the heater to prevent any condensation of sample gas and absorption on the surfaces. The procedure of the gas analysis is as follows. A gas path is first connected to the vacuum pump to make the sample gas fill the whole path. Once the steady state is reached (checked by a manometer attached in the path), the gas path is changed to the GCMS manually by rotating the valve. A part of the extracted sample gas is carried by carrier gas (a high purity of helium: 99.9999%) and introduced into GCMS. A NIST/EPA/NIH mass spectrum library is used for species identification. In this study, two kinds of columns (short and long ones) are employed. The short column (Shimazu CBP1, length 25 m, inner diameter 0.22 mm) is used for detection of PAH, while the long column (J&W Scientific DB-624, length 60 m, inner diameter 0.32 mm) is used for detection of C3/C4 components (as well as benzene). To prevent any damage of GCMS accompanying soot contamination, silica wool is set into the gas path to collect the soot. The silica wool is replaced for every experiment and eliminates any considerable problem (e.g., adsorption of PAH via soot) on gas analyses. A measurement is carried out every 0.5 mm from the lower burner exit on the center axis and a one-dimensional axial profile of species is acquired. The measurement is repeated at least 3 times to

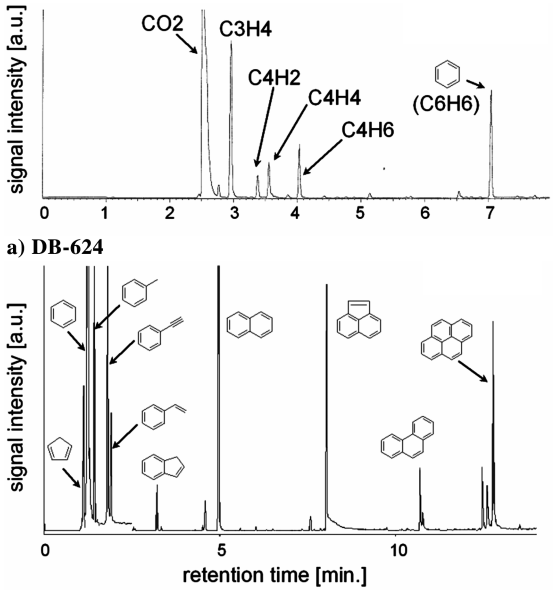

Fig. 5 Typical chromatogram given in gas analyzer with various capillary columns: a) DB-624 (detection up to benzene); b) CBP1 (detection over benzene).

secure reproducibility. According to the verification test performed before the experiment, it is confirmed that the error of measurement is less than 10%. Calibration gas (benzene 298 ppm) is used for the quantification of benzene. A total ionization method [34] is used to calculate the concentration of various species. Before the experiment, the effect of probe insertion on data fluctuation was well checked [by changing the insertion angle and the sampling location in the radial direction (away from the axis)], and it was confirmed that the fluctuation is at most 10%, which is below the system error as stated previously.

Typical chromatogram signals are shown in Fig. 5a as DB-624 and 5b as CBP1. According to the figure, the detection signal shows sufficient signal-to-noise ratio (S/N), suggesting that a high-precision quantitative evaluation could be made.

C. OH–PLIF System

The schematic diagram of an OH–PLIF (planar laser-induced fluorescence) system is shown in Fig. 6. Because the detail of an experiment system is found elsewhere [35], only an outline is described briefly here. A light source consists of a Nd:YAG laser (GCR-230, Spectra Physics, Inc., 10 Hz pulse, 5 ns of pulse width) and a Dye laser (HD-300, Lumonics, Inc.). The second harmonics of the YAG laser (532 nm) are converted into 283.222 nm with the

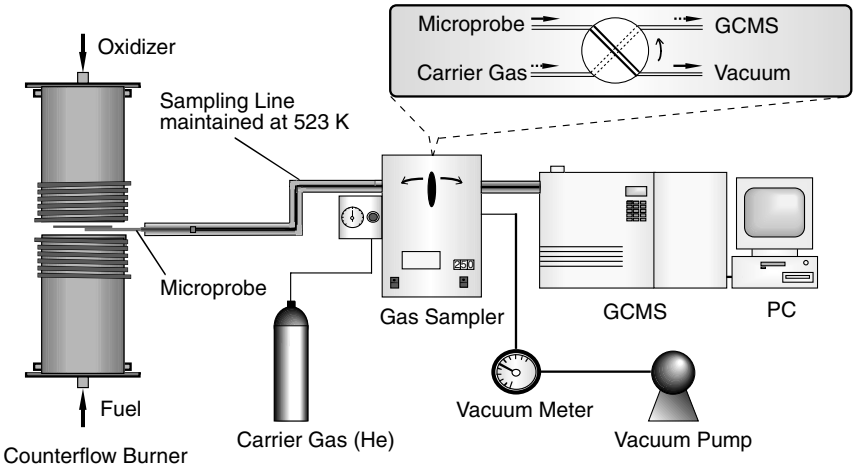

Fig. 4 Schematic illustration of GCMS analyzer system.

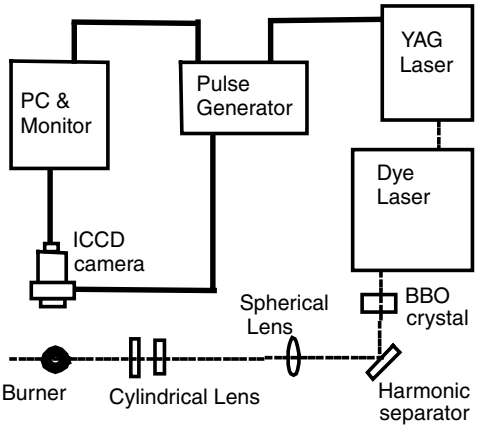

Fig. 6 Schematic illustration of the OH–PLIF system.

combination of a Dye laser and a BBO (β-BaB2O4) crystal. The one equivalent to $A^2\Sigma^+ \leftarrow X^2\Pi$ transition of the (1, 0) band of Q_1 (7) with little temperature dependency is chosen as the absorption wavelength of OH. A laser beam is transformed into a thin sheet by the cylindrical lens and is introduced into the flame. To eliminate the effect of an energy-density profile (Gaussian distribution) of a laser, only the center section extended with the lens is used. The laser power eventually introduced into the flame is about 5–10 mJ.

The charge-coupled device (CCD) camera with an image intensifier (C4272 and C4274, Hamamatsu Photonics Corp.) is used to detect OH fluorescence. The band-pass filter [center 307 nm, full width half maximum (FWHM) 12 nm] is attached ahead of the camera and the exposure time is set as 200 ns, which is the shortest period of this camera, for improvement in the S/N. The pulse generator (DG535, SRS, Inc.) is used for the synchronous control in the system. A one-dimensional axial profile of OH fluorescence intensity (i.e., relative concentration of OH) is acquired using the 10-pixel average near the center axis. The example of a 2-D image obtained by typical OH-PLIF is shown in Fig. 7 (added oxygen amount into the fuel flow is 15%; corresponding equivalence ratio is 10). It turns out that the fluorescence intensity becomes weak in the downstream of the traveling direction of the laser. This is the effect by absorption of OH in the upstream. Though the effect of this absorption is included in the targeted profile, it is possible to argue about a relative change of profile in OH fluorescence intensity by the oxygen addition to a fuel flow.

D. Other Measurement Systems

The thermocouple (platinum–platinum rhodium 13%) is used for the flame temperature measurement. The size of a measurement junction is about 0.3 mm. Correction by radiation loss is made based on Kaskan's correction method [36]. In the correction formula, the Nusselt number is given as 2 (the junction is assumed to be a sphere). When the measurement is performed in a soot-rich zone, it is often seen that soot accumulates on the surface of the junction, which may lead to inaccuracy in local temperature. To reduce this error, before moving the junction to the location of the measurement, the thermocouple is exposed to the blue flame for 5 s or more, and surface soot is removed completely. A measurement is performed every 0.5 mm from the lower burner exit on the center axis and a one-dimensional axial temperature profile is acquired. The measurement is repeated at least 5 times to secure reproducibility. During the measurement, the visible flame shape is slightly deformed due to the nonzero junction volume; hence it is suspected whether or not the measured temperature is dependable. Previously we have performed a numerical simulation with detailed kinetics including up to C2 species (GRI-mech v.2.11) without the soot model under a similar flame condition used in the present study [33]. It has been noted that the maximum measured flame temperature is about 200 K lower than the predicted one, although the good agreement is obtained in the shape of the profile. Soot radiation could reduce flame temperature at least 40 K in standard atmospheric conditions [37].

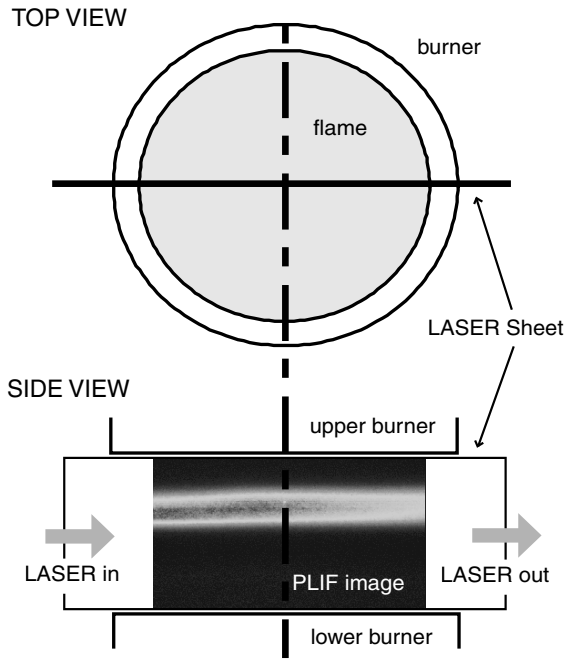

Fig. 7 Example of observed PLIF image.

The luminosity of a flame is measured through the filter, which transmits near 650 nm (the center wavelength of 650 nm, half-band width of 40 nm). The luminosity is a measure of the emissive power of the hot soot (in the flame) and the intensity should be the function of local soot status and the temperature. A one-dimensional luminance profile is acquired using the 10-pixel average around the center axis.

III. Experimental Conditions

In this study, the mixing ratio of an oxidizer gas (mixture of O2/N2) is fixed to 21% of oxygen and 79% of nitrogen by volume. The mixing ratio of a fuel gas (mixture of CH4/O2/N2) is 75% of methane, x% of oxygen, and 75-x% of nitrogen by volume, on the other hand. Here, x represents the added amount of oxygen to a fuel flow and is varied from 0.0 to 15.0 (precisely, $x = 0.0$, 2.5, 5.0, 10.0, and 15.0). Corresponding equivalence ratios are infinity, and 60, 30, 15, and 10, respectively. Initial gas temperature is 300 K and ambient pressure is 0.1 MPa (same as the standard atmospheric condition).

IV. Results and Discussion

A. Responses of 1-D Profiles of Temperature and OH on Oxygen Addition

In Fig. 8, one-dimensional axial profiles of the temperature and OH fluorescence on various oxygen-addition conditions are shown. The location of a luminous flame and a blue flame is added to 8a. According to Fig. 8a, it turns out that temperature increases monotonically in the fuel side. The oxygen addition does not change the shape of the profile, but increases the local temperature uniformly. This trend agrees qualitatively with the results of McEnally and Pfefferle [22] and Saito et al. [38]. Figure 8b shows that OH fluorescence also serves as the maximum in the location which shows the maximum temperature, and a peak in OH fluorescence increases with the increase in the added amount of oxygen. Moreover, the increase in the added amount of oxygen makes the OH fluorescence region broad, suggesting that the oxidation reaction in the fuel side is pronounced. A weak peak in the profile exists near $z = 3.5$ mm and would be due to Raman scattering associated with big soot [39], not the fluorescence from OH.

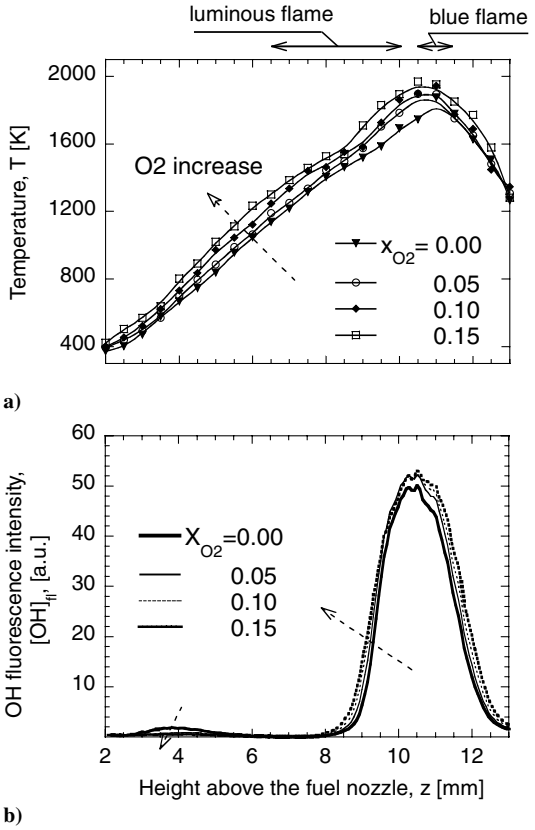

Fig. 8 1-D profiles of a) temperature and b) OH fluorescence signal with various oxygen-addition conditions (0.0–15.0% of O2 addition in the fuel flow). The arrows indicate the changes in increasing the amount of added oxygen.

B. Responses of 1-D Profiles of Flame Luminosity and PAH on Oxygen Addition

Figure 9a shows one-dimensional axial profiles of flame luminance (only near 650 nm), and Figs. 9b–9h show the mole fraction of PAH and cyclopentadiene (C5H6) on various oxygen-addition conditions. According to Fig. 9a, it is shown that the peak value of flame luminance decreases monotonically with the increase in the added amount of oxygen. It is worthwhile to note that the depletion degree becomes small with the increase in the added amount of oxygen. Combined with Fig. 8a, it turns out that the oxygen addition to a fuel flow essentially causes a reduction in soot. As for Figs. 9b–9h, mole fraction profiles of PAH are mostly equivalent, however, that of cyclopentadiene shows a completely opposite trend. The difference might be due to the difference in the formation path of cyclopentadiene: it is generated from a phenyl radical which is mainly produced in the oxidation process of benzene [5,28]. In this sense, the negative correlation between a mole fraction profile of benzene and cyclopentadiene should be acceptable. It is also worthwhile to note that the reduction degree of the peak mole fraction of PAH to the oxygen addition is similar to that of the flame luminance as seen in Fig. 9a, which gives a nonlinear response. Simultaneously, the peak location in the mole fraction profile of PAH shifts to the elevated-temperature zone with the increase in the added amount of oxygen. Mole fractions of PAH are plotted in a temperature plane shown in Fig. 10. As shown in the figure, it is clear that the mole fraction of PAH is *not* determined solely by local temperature. These results convince one that not only temperature but also species profiles are important to predict the local mole fraction of PAH. Again, the figure clearly reveals that PAH production is pronounced only in an elevated-temperature zone (over 1400 K).

After all, to reduce the produced amount of PAH and soot, it is understood that an oxygen addition into the fuel flow works well. Nonetheless, it is also understood that the effectiveness depends on the added amount of oxygen; the maximum reduction rate is experienced in a smaller amount of added oxygen. To discuss more detail about the trend, the change in mole fraction profiles of C3/C4 components, which plays as the source of benzene, is investigated under various oxygen-addition conditions in the next.

C. Responses of 1-D Profiles of C3/C4 on Oxygen Addition

The one-dimensional axial mole fraction profiles of C3/C4 components on various oxygen-addition conditions are shown in Fig. 11. This series of experiments is carried out only with 5% or less of oxygen-addition conditions because our current interest is only in the response with a small amount of the oxygen addition. For comparison purposes, the mole fraction profile of benzene is also shown in Fig. 11e. Here, benzene data shown in Fig. 11e are acquired not with the short column (CBP1) (see Fig. 9b) but with the long one (DB-624) which is used for the detection of C3/C4 components as mentioned previously. As compared with Figs. 9b and 11e, it is known that both are in good agreement qualitatively as well as quantitatively; a slight difference might be due to the error in acquiring a chromatogram signal.

According to the figure, it is shown that the change in the mole fraction profile of C3/C4 components with the oxygen addition is different depending on the species. As seen in Figs. 11a and 11d, for the case of 2.5% of the oxygen addition, the mole fraction profiles of C3H4 and C4H6 stay or even lower as compared to what we observed in the no-oxygen-addition case. However, they become uniformly higher for the case of 5% oxygen addition. It is noted that the increase of local mole fractions of Fig. 11a C3H4 [strongly correlated with C3H3 (propargyl radical)] and Fig. 11b C4H2 in the elevated-temperature zone is more promoted as compared to that in the low temperature zone. This trend is quite similar to the benzene in Fig. 11e. In Fig. 11c, the mole fraction profile of C4H4 is reduced with the increase in the added amount of oxygen, and this trend is somewhat different from other C3/C4 components as well as PAH. The important knowledge acquired here is that the formation/production of the mole fraction of the C3/C4 components is pronounced in an elevated-temperature zone (say, $z > 8.5$ mm) with the increase in the oxygen addition except for that of C4H4. Especially, the increase of the mole fraction of C3H4 in the elevated-temperature zone is remarkable as compared to the others and it is expected that C3H4 ($\sim$C3H3) plays a role in the promotion of PAH and soot formation observed here.

D. Appearance of "Leveling-Off" Trend in Averaged Mole Fraction of Benzene with Oxygen Addition

In this section, we concentrate on the formation as well as the consumption processes of benzene to reveal the reason of the appearance of the "leveling-off" trend in the averaged mole fraction of benzene (see Fig. 12) connected with the change of the profile with the oxygen addition as seen in Fig. 9. First, let us start with the consumption process of benzene. There are two possible paths to be considered for benzene consumption; one is the growth to larger PAH, and the other is oxidation. Recalling Fig. 9, it has been observed that the mole fractions of PAH are reduced by an oxygen addition, suggesting that the PAH formation is also suppressed with an oxygen addition. Simultaneously, this result indicates that the main consumption path of benzene would be the oxidation, not the growth to larger PAH. Candidates of oxidizing matter for PAH are O2, H, OH, and O [5,14,16,28]. Among those, the O atom hardly exists in the fuel side (normally its mole fraction is 3 orders of magnitude smaller than others in the nonpremixed combustion of typical hydrocarbon fuel [33]). Hence, the main oxidizer components are considered to be O2, H, and OH. According to the currently available kinetics models, the following three reactions are mainly considered for the oxidation of benzene [5,16,22,29]:

$C6H6(+H/H2) \Rightarrow C6H5(+O2) \Rightarrow C6H5O \Rightarrow C5H5$

$C6H6(+OH) \Rightarrow C6H5OH(+OH) \Rightarrow C6H5O \Rightarrow C5H5$

$C6H6(+O) \Rightarrow C6H6O \Rightarrow C5H6(+H/OH) \Rightarrow C5H5$

C5H5 (cyclopentadienyl radical, which has a strong correlation to C5H6 [28]), as a product of benzene oxidation, would be further

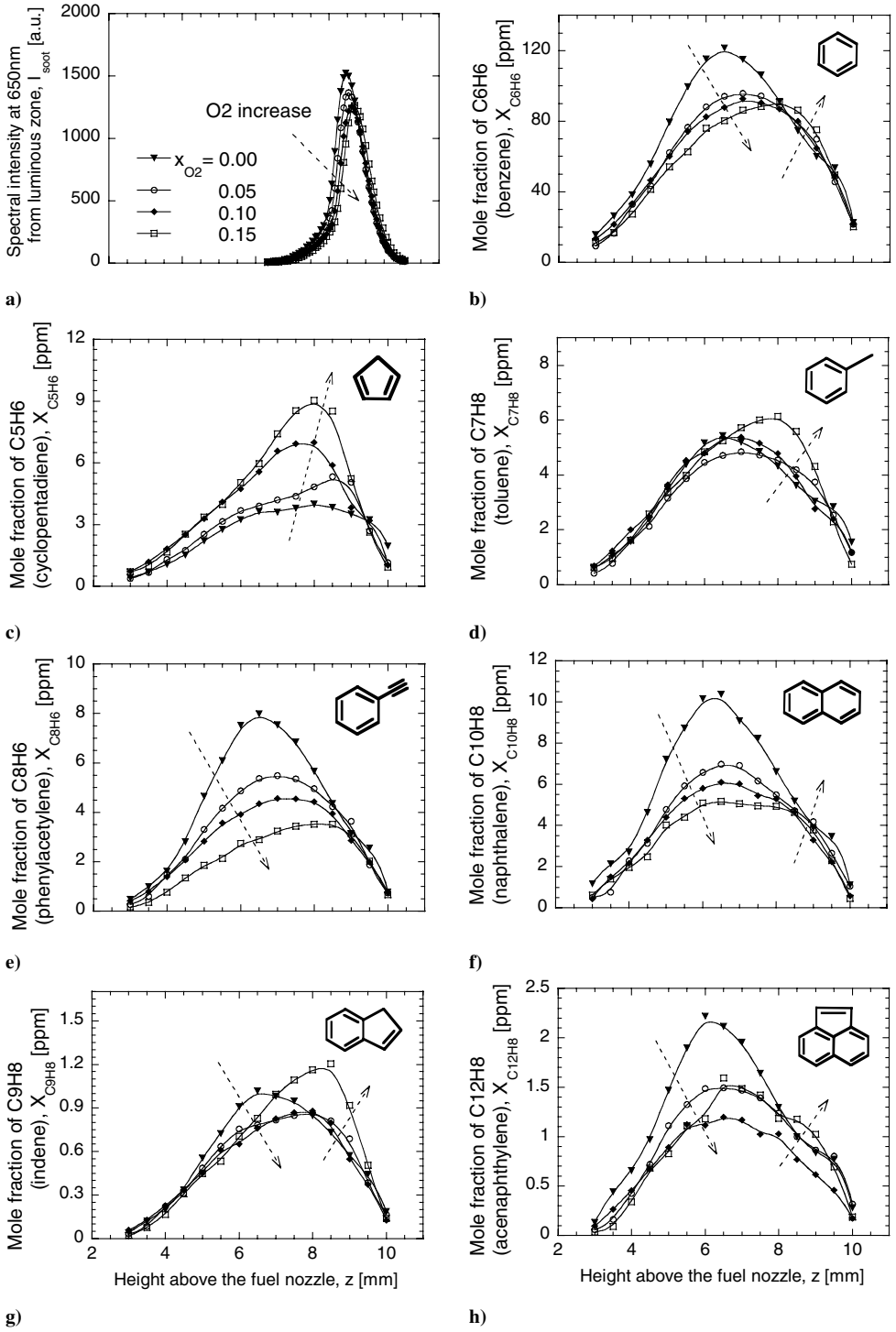

Fig. 9 1-D profiles of a) flame luminosity at 650 nm and b)–h) mole fractions of PAH (up to two rings) with various oxygen-addition conditions (0.0–15.0% of O2 addition in the fuel flow). Arrows indicate the changes in increasing the amount of added oxygen.

oxidized or decomposed to lower-class hydrocarbons (C2/C3/C4) through the following reactions:

C5H5(+O) ⇒ C4H3 ⇒ C4H2

C5H5(+OH) ⇒ C4H4(+H) ⇒ C3H4 ⇒ C3H3

⇒ C4H4(+O) ⇒ C3H4 ⇒ C2H2

C5H5(+OH) ⇒ C5H4OH(+H) ⇒ CH2O, C2H2

⇒ C5H4OH ⇒ C5H4O (+O or thermal decomposition) ⇒ C2H2

C5H4OH(+O) ⇒ *n*–C4H5 ⇒ *i*–C4H5(+OH) ⇒ C4H4(+H) ⇒ *i*–C4H3 ⇒ C4H2

⇒ *i*–C4H5(thermal decomposition) ⇒ C2H2

One can consider that C5H5 will be consumed to form larger PAH [e.g., C5H5 + C5H5 ⇒ C10H8 (naphthalene: 2 rings) + 2H, C5H5 + C9H7 (indenyl) ⇒ C14H10 (phenanthrene: 3 rings)+ 2H] [15] besides the oxidative degradation shown previously. However, if it is correct, the decrement of the benzene with the oxygen addition should be equal (at least equivalent) to the sum of the increment of larger PAH and cyclopentadiene. Figure 9 clearly shows that an absolute increment of the mole fraction of cyclopentadiene with an oxygen addition is small and the mole fractions of larger PAH are actually decreased rather than increased. Therefore, it could be appropriate to recognize that benzene goes to a low class of hydrocarbon through C5H5 via oxidation when the oxygen is added in the fuel flow.

According to Wang and Frenklach [16], the reaction which gives a direct conversion from benzene to C3H3 does not exist. In general,

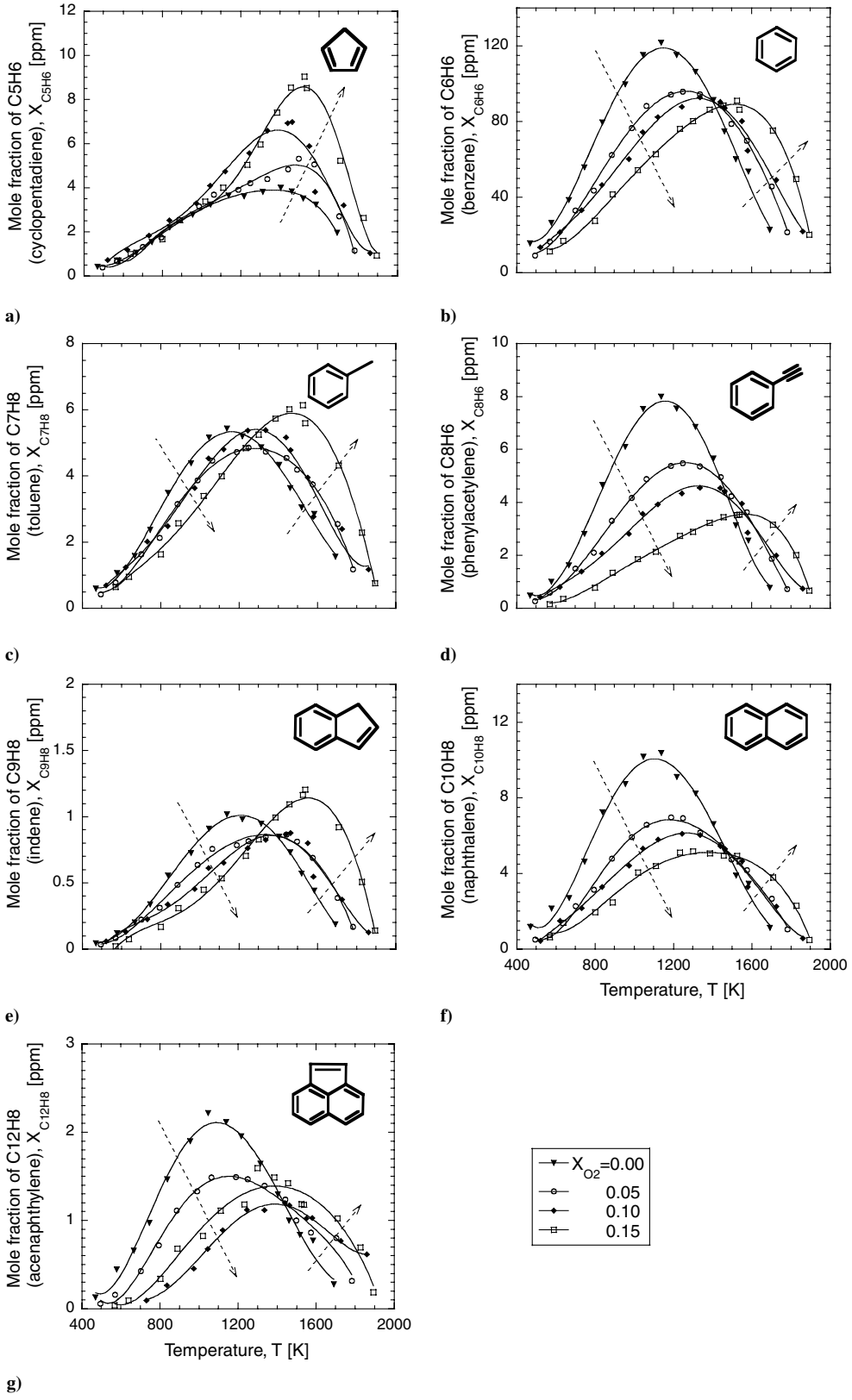

Fig. 10 Produced mole fraction of PAH (up to two rings) as a function of field temperature with various oxygen-addition conditions a)–g) (0.0–15.0% of O2 addition in the fuel flow). Arrows indicate the changes in increasing the amount of added oxygen.

C3H3 is produced from C2H2 (by the reaction with CH and CH2 [16,29]), or C4 components (by the reaction with H [5,16]). In the oxidation reaction of the benzene shown above, C4 components are produced first, then C3H3 follows (C6H6 $\Rightarrow$ C4 compounds $\Rightarrow$ C3H3). It is important to point out that OH and O are essential to this reaction to occur (to form C3H3) in the fuel side and they are available only in the elevated-temperature zone. On the other hand, C2H2 as the reactant of formation reaction of C3H3 could exist widely in the fuel side even in a low-temperature zone. Because H is produced by the fuel decomposition reactions, it can also exist in a low-temperature zone. Thus, the main production path of C3H3 could be different in the temperature level: the C2H2 originated path

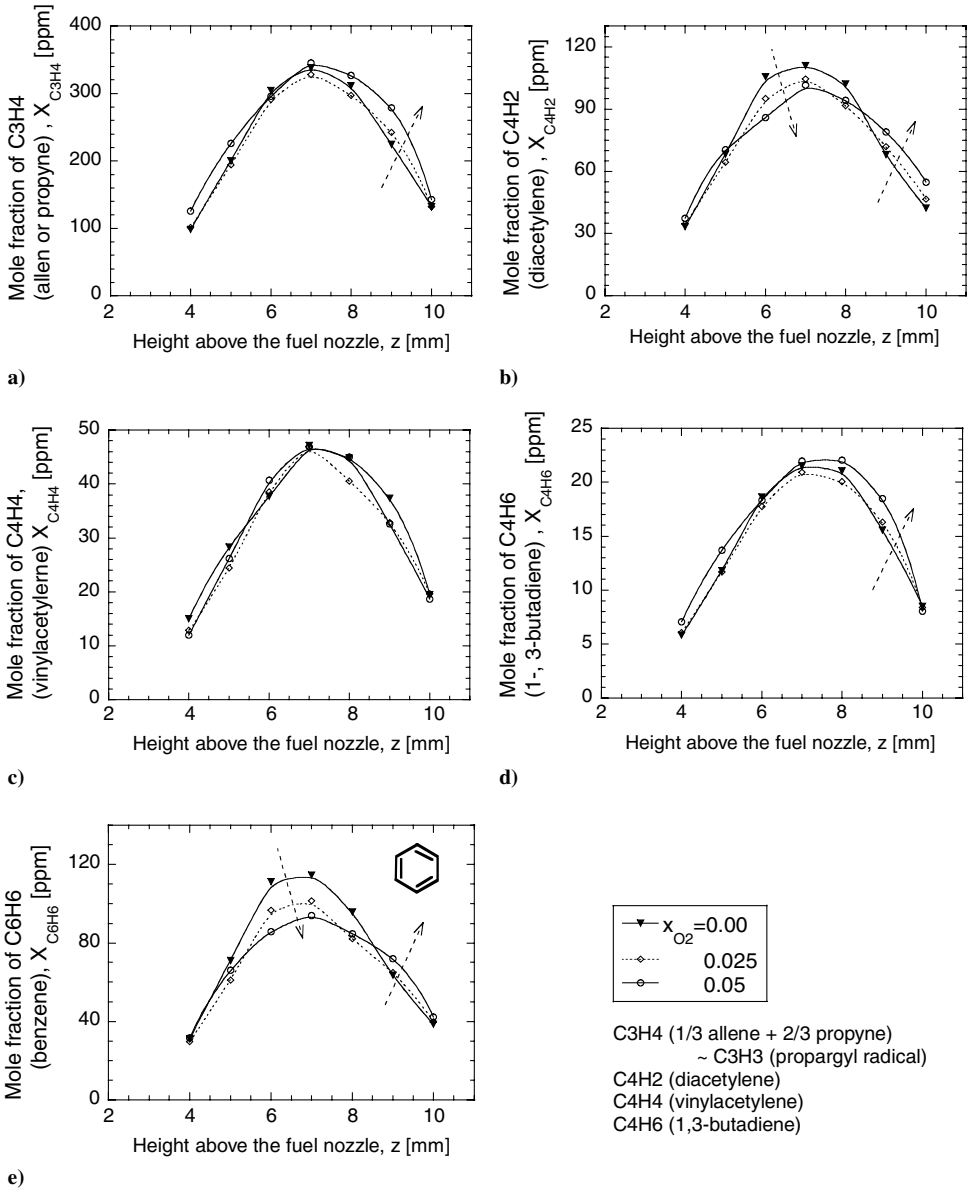

Fig. 11 1-D profiles of mole fractions of C3/C4 species with various oxygen-addition conditions a)–e) (selected only 0.0–5.0% of O2 addition in the fuel flow) for comparison purposes. Arrows indicate the changes in increasing the amount of added oxygen.

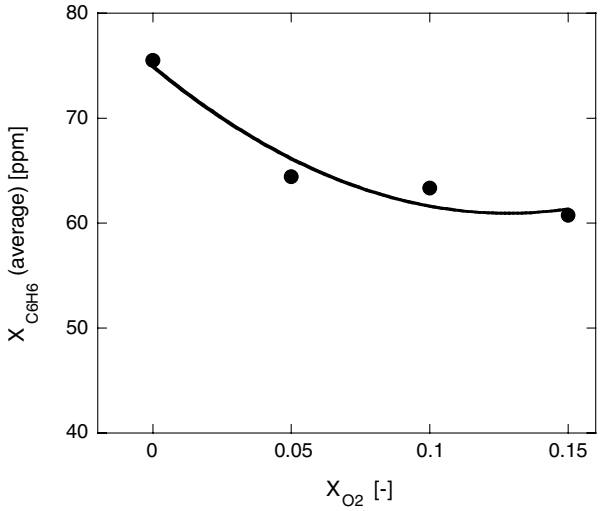

Fig. 12 Change of averaged benzene mole fraction [X_{C6H6} (average)] in added oxygen amount in the fuel flow (X_{O2}).

would be preferred in the low-temperature zone and the C4 component originated path would be done in the elevated-temperature zone.

Benzene formation mainly consists of a recombination reaction of C3H3 and a reaction of C2 and C4 as shown here:

C3H3(+C3H3) ⇒ C6H6 (benzene)

n–C4H*x*(+C2H2) ⇒ C6H6 or C6H5

In a recent model study, it was revealed that these rates of reaction have a different sensibility to temperature: the former has higher temperature sensitivity at higher temperature than the latter [29]. Although the C2/C3/C4 components are reactants to benzene formation, they are also products over benzene oxidation as stated previously. Therefore, to explain the observed result well, one can consider that benzene oxidation with oxygen addition appears more notably than formation (so that benzene is consumed overall) in the low-temperature zone, and just reversed in the elevated-temperature zone. If the previously described difference in temperature sensitivity is taken into account, it is suspected that the promotion of benzene formation is led by C3H3 in the elevated-temperature zone.

To convince the above prediction, numerical simulation for the corresponding conditions is attempted. Details of the numerical technique are found elsewhere [33]; thermal properties are given by the CHEMKIN database, while transport properties are given by

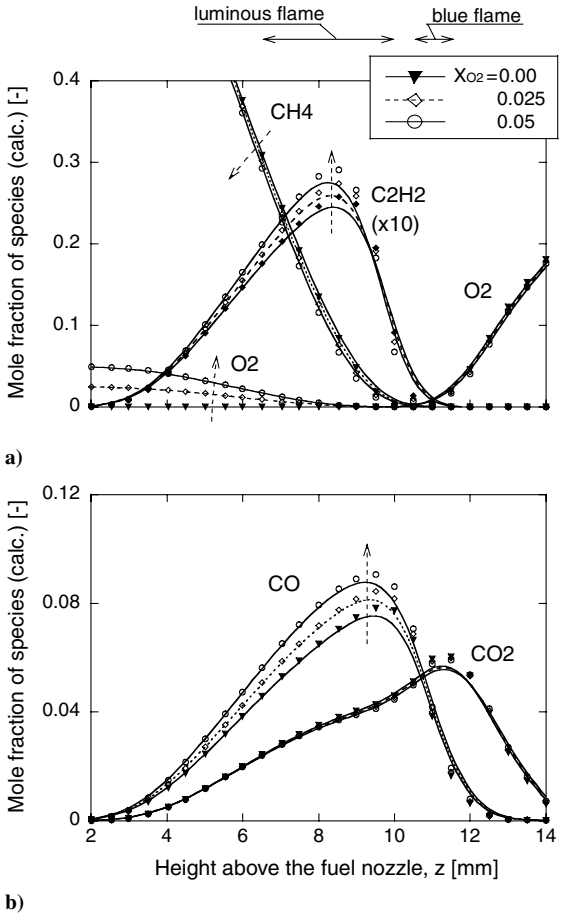

Fig. 13 1-D profiles of predicted mole fractions a), b) of major species (CH4, O2, C2H2, CO, CO2) by applying GRI-mech v.2.11 with various oxygen-addition conditions (selected only 0.0–5.0% of O2 addition in the fuel flow). Arrows indicate the changes in increasing the amount of added oxygen.

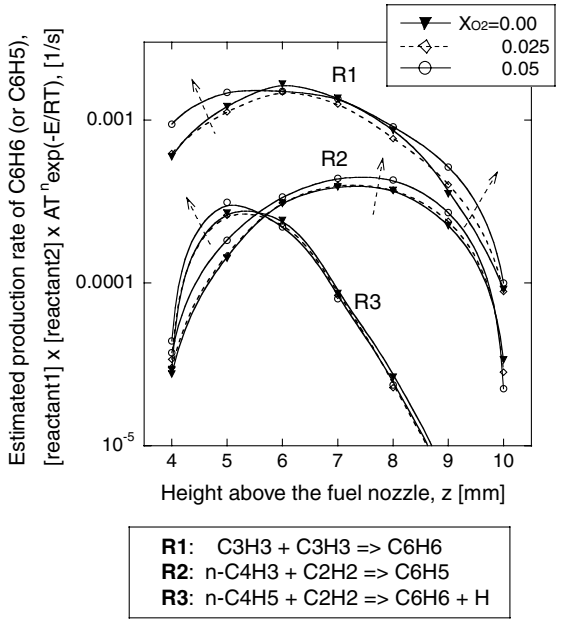

Fig. 14 Estimated 1-D profiles of benzene production rate with various oxygen-addition conditions (selected only 0.0–5.0% of O2 addition in the fuel flow). Arrows indicate the changes in increasing the amount of added oxygen.

Smooke's simplified transport model [40]. The applied kinetics model is GRI-mech v.2.11 because it is dependable to predict a low class of hydrocarbons. Although the kinetics model to handle the heavier hydrocarbons (larger than C3 such as PAH) is available, it is not sure that the model is really dependable for the present condition. At this stage, we apply GRI-mech v.2.11 to predict up to C2 species which are not given by experiment, and then estimate the PAH production rate with the conjunction of the "predicted" mole fraction of C2 species and the "measured" mole fraction of C3/C4. Figure 13 shows a predicted flame structure of a major species (CH4, O2, C2H2, CO, CO2). It is understood that the mole fraction of C2H2 and CO is increased but that of CO2 remains as the added amount of oxygen is increased, implying that the oxygen addition into the fuel flow promotes the combustion intermediate. With use of the predicted mole fraction of species (C2H2), the production rates of benzene (or phenyl) through represented C3/C4 reactions (R1: C3H3 + C3H3 ⇒ C6H6, R2: *n*–C4H3 + C2H2 ⇒ C6H5, R3: *n*–C4H5 + C2H2 ⇒ C6H6 + H) are estimated. The measured temperature and mole fraction of C3/C4 are used for the estimation, and kinetics constants are referred from the literature [16]. Because unstable intermediates (such as C3H3, *n*–C4H3, *n*–C4H5) could not be measured in the present system, we assume that their mole fractions are the same as stable ones (such as C3H4, *n*–C4H4, *n*–C4H6). Because a strong correlation between the unstable intermediate and the stable one has been pointed out as stated previously [41], this assumption does not destroy the qualitative accuracy in further discussion. The result is shown in Fig. 14, indicating that R1 and R2 are responsible for the benzene production in the elevated-temperature zone as found in the experiment.

Consequently, the reason of the appearance of the leveling-off trend in the averaged mole fraction of benzene (again, see Fig. 12) and the change of its profile with the oxygen addition will be summarized as follows. Benzene is oxidized in the low-temperature zone with an oxygen addition, and it changes to the C2/C3/C4 components through C5H5. Among those, C4 components are converted to C3H3 in an elevated-temperature zone (over 1400 K), and produced C3H3 returns to benzene through the recombination reaction there. The C4 species reacts with C2H2 to form benzene. The field temperature also rises by the oxygen addition, so that the benzene formation by the recombination of C3H3 and C4/C2 reactions is enhanced as the increase of the added amount of oxygen. As a result, the depletion degree of benzene (and following PAH) is reaching the ceiling and the shape of the profile is modified (peaks shift to the elevated-temperature zone) with the increase in oxygen addition.

E. Oxygen (Premixing) Role on Benzene Formation or Consumption

The conditions of a small (here 2.5%) oxygen addition have the largest inhibition over benzene formation as pointed out previously. It can bring about 10% of emission reduction on the conditions investigated in this study. As for the amount of the oxygen addition of this level (it is 60 at an equivalence ratio), it is interesting to point out that it is almost equal to the value (it is about 100 at a considerable equivalence ratio) attained by the oxygen entrained from the quench area in a 2-D jet nonpremixing (diffusion) flame [37]. To attain the emission control beyond it, special treatments, such as removing C3H3/*n*–C4H3/C2H2 in an elevated-temperature zone, would be necessary.

In the case of a 2-D jet nonpremixing (diffusion) flame, the mole fraction of benzene decreases with the increase in the amount of the oxygen addition, and the leveling-off trend is not observed [22]. The discrepancy with the present results should be based on the difference in the dimension of an object flame (2-D vs 1-D). When a certain "flamelet" in the laminar nonpremixing (diffusion) flame is considered, it can be reproduced via a counterflow nonpremixing (diffusion) flame with certain boundary conditions. It must be noted that boundary conditions in the fuel and oxidizer side would not be the one at the burner exit nor the one far away (pure oxidizer compound), respectively. In the downstream flamelet, fuel/oxidizer sides will be diluted and will be preheated, because the hot products (for example, CO, H2, CO2, H2O, etc.) generated in the upstream flamelet are flowed and modified as the gas components there. Therefore, soot emission characteristics along the center axis may

vary according to the burner size, flow rate (flame length), surrounding flow rate, and so on. Moreover, by a jet flame, an entrain of oxygen through the quenching gap cannot be eliminated. To summarized, it is rather natural to show a different emission tendency on the oxygen addition to 2-D and 1-D flames.

In this study, one possible thought to explain an experimental result is proposed; that is, the effect of the oxygen addition to a fuel flow would contribute simultaneously to consume benzene by oxidation and to produce C3/C4 as a benzene oxidation product, and increase in flame temperature. Recombination reactions of C3H3 and C4/C2 to form benzene are both pronounced in higher flame temperature, resulting in two competing reaction paths for benzene formation and consumption with an oxygen addition. The latter comes into play as a role to give the observed leveling-off trend in the averaged mole fraction of benzene with a little oxygen addition into the fuel flow. However, this is just the first guess obtained with conditions considered here. In our flames, there is too much fuel (over 85%) in a fuel flow, and it is suspected that a considerable amount of fuel remains as unburned (this is why we observe soot in the flame). This must be the reason why the flame temperature rises with the oxygen addition to promote benzene formation, resulting in the above-mentioned leveling-off trend. In this sense, it is not clear whether the leveling-off tendency always appears, for example, the case where the oxygen addition does not change the temperature field. Further experimental study would be necessary to make clear the generality of the above explanation and oxygen role added into the fuel flow. Finally, it should be stressed that the current experimental data would be useful as the validation source in further development of kinetics modeling, because this paper gives the simple 1-D mole fraction profile of PAH as well as C3/C4 components.

V. Conclusions

The effects of an oxygen addition into the *fuel* flow in counterflow, methane–air nonpremixed (diffusion) flames on the PAH formation character are examined experimentally. Measurement of mole fraction profiles of C3/C4 components and PAH by gas chromatograph-mass spectrometer (GCMS), temperature profile by thermocouple, OH fluorescence profile by laser-induced fluorescence (LIF), and flame luminosity by filtered camera at 650 nm are performed. An added amount of oxygen into the fuel flow is varied from 0% (pure diffusion flame) to 15% by volume. A corresponding equivalence ratio of the fuel mixture is in the range from 10 to infinity, ensuring that the mixture cannot propagate itself (out of the propagation range). It is understood that the decrease of the total amount of PAH can be attained by the oxygen addition into the fuel flow. Field temperature is increased and the mole fraction of PAH does not decrease much with the increase of the added oxygen amount. Furthermore, a decrement in the averaged mole fraction of benzene shows the leveling-off trend with a slight-premixing treatment, suggesting that a little amount of the oxygen into the fuel flow could give the most efficient reduction of PAH. It is considered that reactions of propargyl radical (C3H3) recombination and *n*–C4H3 with C2H2 play an important role in giving the leveling-off trend observed in this study. One possible thought to explain an experimental result is proposed: the effect of the oxygen addition to a fuel flow would contribute simultaneously to consume benzene by oxidation with H and OH and to produce the intermediate radicals (such as C3H3, *n*–C4H3), and increase in flame temperature. In the elevated-temperature zone (over 1400 K), benzene production through propargyl recombination and C4-acetylene reactions is pronounced to give the observed leveling-off trend in the decrement of mole fraction of benzene (and so to other PAH). Current experimental data would be useful for further development of kinetics modeling for their validation purpose.

Acknowledgments

This work is supported by the Showa Shell Sekiyu Foundation for the Promotion of Environmental Research and the Steel Industry Foundation for the Advancement of Environmental Protection Technology. Technical and professional advice provided by T. Takeno (Meijo University) and M. Nishioka (University of Tsukuba) was extremely helpful. Yuji Nakamura expresses his sincere thanks for their help in conducting this study.

References

[1] Stehling, F. C., Frazee, J. D., and Anderson, R. C., "Carbon Formation from Acetylene," *Proceedings of the Combustion Institute*, Vol. 6, 1956, pp. 247–254.

[2] Scully, D. B., and Davies, R. A., "Carbon Formation from Aromatic Hydrocarbons," *Combustion and Flame*, Vol. 9, No. 2, 1965, pp. 185–191.
doi:10.1016/0010-2180(65)90064-7

[3] Davies, R. A., and Scully, D. B., "Carbon Formation from Aromatic Hydrocarbons II," *Combustion and Flame*, Vol. 10, No. 2, 1966, pp. 165–170.
doi:10.1016/0010-2180(66)90064-2

[4] Haynes, B. S., and Wagner, H. G., "Soot Formation," *Progress in Energy and Combustion Science*, Vol. 7, No. 4, 1981, pp. 229–273.
doi:10.1016/0360-1285(81)90001-0

[5] Bittner, J. D., and Howard, J. B., "Composition Profiles and Reaction Mechanisms in a Near-Sooting Premixed Benzene/Oxygen/Argon Flame," *Proceedings of the Combustion Institute*, Vol. 18, 1981, pp. 1105–1116.

[6] Backhorn, H., *Soot Formation in Combustion*, Springer–Verlag, New York, 1994, pp. 9–104.

[7] Kennedy, I. M., "Models of Soot Formation and Oxidation," *Progress in Energy and Combustion Science*, Vol. 23, No. 2, 1997, pp. 95–132.
doi:10.1016/S0360-1285(97)00007-5

[8] Ritcher, H., and Howard, J. B., "Formation of Polycyclic Aromatic Hydrocarbons and Their Growth to Soot—A Review of Chemical Reaction Pathways," *Progress in Energy and Combustion Science*, Vol. 26, Nos. 4–6, 2000, pp. 565–608.
doi:10.1016/S0360-1285(00)00009-5

[9] Ishiguro, T., Takatori, Y., and Akihama, K., "Microstructure of Diesel Soot Particles Probed by Electron Microscopy: First Observation of Inner Core and Outer Shell," *Combustion and Flame*, Vol. 108, Nos. 1–2, 1997, pp. 231–234.
doi:10.1016/S0010-2180(96)00206-4

[10] Oktem, B., Tolocka, M. P., Zhao, B., Wang, H., and Johnston, M. V., "Chemical Species Associated with the Early Stage of Soot Growth in a Laminar Premixed Ethylene-Oxygen-Argon Flame," *Combustion and Flame*, Vol. 142, No. 4, 2005, pp. 364–373.
doi:10.1016/j.combustflame.2005.03.016

[11] Kennedy, I. M., Yam, C., Rapp, D. C., and Santoro, R. J., "Modeling and Measurement of Soot and Species in a Laminar Diffusion Flame," *Combustion and Flame*, Vol. 107, No. 4, 1996, pp. 368–382.
doi:10.1016/S0010-2180(96)00092-2

[12] Frenklach, M., and Warnatz, J., "Detailed Modeling of PAH Profiles in a Sooting Low-Pressure Acetylene Flame," *Combustion Science and Technology*, Vol. 51, Nos. 4–6, 1987, pp. 265–283.
doi:10.1080/00102208708960325

[13] Miller, J. A., and Melius, C. F., "Kinetic and Thermodynamic Issues in the Formation of Aromatic Compounds in Flames of Aliphatic Fuels," *Combustion and Flame*, Vol. 91, No. 1, 1992, pp. 21–39.
doi:10.1016/0010-2180(92)90124-8

[14] Alexiou, A., and Williams, A., "Soot Formation in Shock-Tube Pyrolysis of Toluene, Toluene-Methanol, Toluene-Ethanol, and Toluene-Oxygen Mixtures," *Combustion and Flame*, Vol. 104, Nos. 1–2, 1996, pp. 51–65.
doi:10.1016/0010-2180(95)00004-6

[15] Marinov, N. M., Castaldi, M. J., Melius, C. F., and Tsang, W., "Aromatic and Polycyclic Aromatic Hydrocarbon Formation in a Premixed Propane Flame," *Combustion Science and Technology*, Vol. 128, Nos. 1–6, 1997, pp. 295–342.
doi:10.1080/00102209708935714

[16] Wang., H., and Frenklach, K., "A Detailed Kinetic Modeling Study of Aromatic Formation in Laminar Premixed Acetylene and Ethylene Flames," *Combustion and Flame*, Vol. 110, Nos. 1–2, 1997, pp. 173–221.
doi:10.1016/S0010-2180(97)00068-0

[17] Marinov, N. K., Pitz, W. J., Westbrook, C. K., Vincitore, A. M., Castaldi, M. J., and Senkan, S. M., "Aromatic and Polycyclic Aromatic Hydrocarbon Formation in a Laminar Premixed n-Butane Flame," *Combustion and Flame*, Vol. 114, Nos. 1–2, 1998, pp. 192–213.
doi:10.1016/S0010-2180(97)00275-7

[18] Hwang, J. Y., Lee, W., Kang, H. G., and Chung, S. H., "Synergistic Effect of Ethylene-Propane Mixture on Soot Formation in Laminar Diffusion Flames," *Combustion and Flame*, Vol. 114, Nos. 3–4, 1998, pp. 370–380. doi:10.1016/S0010-2180(97)00295-2

[19] McEnally, C. S., and Pfefferle, L. D., "Species and Soot Concentration Measurements in a Methane/Air Nonpremixed Flame Doped with C4 Hydrocarbons," *Combustion and Flame*, Vol. 115, Nos. 1–2, 1998, pp. 81–92.

[20] McEnally, C. S., and Pfefferle, L. D., "Experimental Study of Nonfuel Hydrocarbon Concentrations in Coflowing Partially Premixed Methane/Air Flames," *Combustion and Flame*, Vol. 118, No. 4, 1999, pp. 619–632. doi:10.1016/S0010-2180(99)00017-6

[21] McEnally, C. S., and Pfefferle, L. D., "Experimental Study of Nonfuel Hydrocarbon and Soot in Coflowing Partially Premixed Ethylene/Air Flames," *Combustion and Flame*, Vol. 121, No. 4, 2000, pp. 575–592. doi:10.1016/S0010-2180(99)00174-1

[22] McEnally, C. S., and Pfefferle, L. D., "The Effects of Slight Premixing on Fuel Decomposition and Hydrocarbon Growth in Benzene-Doped Methane Nonpremixed Flames," *Combustion and Flame*, Vol. 129, No. 3, 2002, pp. 305–323. doi:10.1016/S0010-2180(02)00347-4

[23] Inal, F., and Senkan, S., "Effects of Equivalence Ratio on Species and Soot Concentrations in Premixed N-Heptane Flames," *Combustion and Flame*, Vol. 131, Nos. 1–2, 2002, pp. 16–28. doi:10.1016/S0010-2180(02)00388-7

[24] Granata, S., Faravelli, T., Ranzi, E., Olten, N., and Senkan, S. M., "Kinetic Modeling of Counterflow Diffusion Flames of Butadiene," *Combustion and Flame*, Vol. 131, No. 3, 2002, pp. 273–284. doi:10.1016/S0010-2180(02)00407-8

[25] Xu, F., El-Leathy, A. M., Kim, C. H., and Feath, G. M., "Soot Surface Oxidation in Hydrocarbon/Air Diffusion Flames at Atmospheric Pressure," *Combustion and Flame*, Vol. 132, Nos. 1–2, 2003, pp. 43–57. doi:10.1016/S0010-2180(02)00459-5

[26] D'Anna, A., and Kent, J. H., "Aromatic Formation Pathways in Non-Premixed Methane Flames," *Combustion and Flame*, Vol. 132, No. 4, 2003, pp. 715–722. doi:10.1016/S0010-2180(02)00522-9

[27] Atakan, B., Lamprecht, A., and Kohse-Hoinghaus, K., "An Experimental Study of Fuel-Rich 1,3-Pentadiene and Acetylene/Propane Flames," *Combustion and Flame*, Vol. 133, No. 4, 2003, pp. 431–440. doi:10.1016/S0010-2180(03)00040-3

[28] Dupont, L., El Bakali, A., Pauwels, J.-F., Da Costa, I., Meunier, P., and Richter, H., "Investigation of Stoichiometric Methane/Air/Benzene (1.5%) and Methane/Air Low Pressure Flames," *Combustion and Flame*, Vol. 135, Nos. 1–2, 2003, pp. 171–183. doi:10.1016/S0010-2180(03)00158-5

[29] Skjoth-Rasmussen, M. S., Glarborg, P., Ostberg, M., Johannessen, J. T., Livbjerg, H., Jensen, A. D., and Christensen, T. S., "Formation of Polycyclic Aromatic Hydrocarbons and Soot in Fuel-Rich Oxidation of Methane in a Laminar Flow Reactor," *Combustion and Flame*, Vol. 136, Nos. 1–2, 2004, pp. 91–128. doi:10.1016/j.combustflame.2003.09.011

[30] Lee, S. M., Yoon, S. S., and Chung, S. H., "Synergistic Effect on Soot Formation in Counterflow Diffusion Flames of Ethylene-Propane Mixtures with Benzene Addition," *Combustion and Flame*, Vol. 136, No. 4, 2004, pp. 493–500. doi:10.1016/j.combustflame.2003.12.005

[31] Yamaguchi, T., Nakamura, Y., Zhao, D., and Yamashita, H., "Experimental Study on PAHs Formation Characteristics in Counterflow Diffusion Flame," *Transactions of the Tokai Institute of Fluid and Heat Engineering*, Vol. 38, No. 1, 2003, pp. 29–38 (in Japanese).

[32] Hasegawa, Y., Yamaguchi, T., Nakamura, Y., Zhao, D., and Yamashita, H., "Effects of Benzene Addition on PAHs Formation Characteristics in a Counterflow Diffusion Flame," *Proceedings of the 19th International Colloquium on Dynamics of Explosion and Reactive Systems, Hakone Japan*, 2003.7, Fr2-3-2 [CD-ROM].

[33] Hasegawa, Y., Nakamura, Y., and Yamashita, Y., "Effects of Oxygen Concentration on PAHs Formation in a Counterflow Diffusion Flame," *Transactions of the Japan Society of Mechanical Engineers*, Vol. 71, No. 705, 2005, pp. 1475–1482 (in Japanese).

[34] Fitch, W. L., and Sauter, A. D., "Calculation of Relative Electron Impact Total Ionization Cross Section for Organic Molecules," *Analytical Chemistry*, Vol. 55, No. 6, 1983, pp. 832–835. doi:10.1021/ac00257a006

[35] Yamamoto, N., Nakamura, Y., Satomi, T., Hayashi, N., Yamashita, H., and Zhao, D., "Study on OH Structure in Turbulent Premixed Flames by PLIF," *Proceedings of the 19th International Colloquium on Dynamics of Explosion and Reactive Systems, Hakone Japan*, 2003.7, Mo1-3-3 [CD-ROM].

[36] Kaskan, W. E., "The Dependence of Flame Temperature on Mass Burning Velocity," *Proceedings of the Combustion Institute*, Vol. 6, 1957, pp. 134–143.

[37] Zhu, X. L., and Gore, J. P., "Radiation Effects on Combustion and Pollutant Emissions of High-Pressure Opposed Flow Methane/Air Diffusion Flames," *Combustion and Flame*, Vol. 141, Nos. 1–2, 2005, pp. 118–130. doi:10.1016/j.combustflame.2004.12.012

[38] Saito, K., Williams, F. A., and Gordon, A. S., "Effects of Oxygen on Soot Formation in Methane Diffusion Flames," *Combustion Science and Technology*, Vol. 47, Nos. 3–4, 1986, pp. 117–138. doi:10.1080/00102208608923869

[39] Vincitore, A. M., and Senkan, S. M., "Experimental Studies of the Micro-Structure of Opposed Flow Diffusion Flames: Methane," *Combustion Science and Technology*, Vol. 130, Nos. 1–6, 1997, pp. 233–246. doi:10.1080/00102209708935744

[40] Smooke, M. D., *Reduced Kinetic Mechanisms and Asymptotic Approximations for Methane-Air Flames*, Springer–Verlag, New York, 1991, pp. 1–28.

[41] Miller, J. A., and Melius, C. F., "Kinetic and Thermodynamic Issues in the Formation of Aromatic Compounds in Flames of Aliphatic Fuels," *Combustion and Flame*, Vol. 91, No. 6, 1992, pp. 21–39. doi:10.1016/0010-2180(92)90124-8

A. Gupta
Associate Editor